ORGANIC CHEMISTRY FRONTIERS

CCS 中国化学会 CHINESE CHEMICAL SOCIETY

SIOC 1950

ROYAL SOCIETY OF CHEMISTRY

RESEARCH ARTICLE

Cite this: *Org. Chem. Front.*, 2021, **8**, 4078

J-aggregation induced emission enhancement of BODIPY dyes *via* H-bonding directed supramolecular polymerization: the importance of substituents at boron†

Yongjie Zhang, ‡[a] Siyuan Yuan,‡[a] Ping Liu,[a] Lei Jing,[a] Hongfei Pan,[a] Xiang-Kui Ren *[a,b] and Zhijian Chen *[a,b]

Received 3rd April 2021,
Accepted 19th May 2021

DOI: 10.1039/d1qo00520k

rsc.li/frontiers-organic

Two new boron-dipyrromethene (BODIPY) dyes **1b** and **1c**, bearing two uracil units at the 2,6-positions and solubilizing alkyne groups at boron atoms, were synthesized and characterized. The UV/Vis absorption and fluorescence spectroscopic studies indicated that in nonpolar solvents these BODIPY dyes supramolecularly polymerized into J-aggregates, which exhibited outstanding optical properties, such as narrowed absorption and emission bands with reduced fluorescence lifetime and increased quantum yields with respect to that for monomers. The mechanism of the polymerization of **1b** and **1c** was analysed by temperature- and concentration-dependent spectroscopy and studied with a nucleation–elongation model. Measurements of concentration-dependent ^{1}H NMR and AFM demonstrated the H-bonding directed self-assembly of J-aggregates of dyes **1b** and **1c**, which led to the formation of one-dimensional nanowires of these dyes. Further molecular modelling studies and calculations based on exciton theory indicated that the bulky alkyne substituents at boron atoms effectively hindered the close contact between the π-faces of BODIPY chromophores, implying that the appropriate segregation of supramolecular polymer chains could be crucial for the aggregation-induced emission enhancement (AIEE) for this class of BODIPY dyes, as compared with the fluorescence quenching observed for the J-aggregates of BODIPY **1a** bearing F atoms at boron in our previous report.

Introduction

J-aggregates of functional dyes have been investigated extensively in multidisciplinary research since their serendipitous discovery in the 1930s.[1] The most attractive features of these dye aggregates are their remarkable optical properties caused by strong excitonic coupling of the dye units and their applications in important fields such as artificial light harvesting[2] and sensitization in colour photography.[3] To form J-aggregates, molecular packing with strong slippage of the chromophores is crucial and supramolecular principles have been adopted for rational control of the spatial arrangement of the dye molecules. For example, amphiphilically modified carbocyanine dyes have been reported to form highly ordered nanotubular or ribbon-like J-aggregates in early studies.[4] More recently, Würthner *et al.* have developed a series of highly fluorescent J-aggregates based on perylene bisimide dyes through supramolecular design,[5] in which the head-to-tail alignment of chromophores is directed by imide hydrogen-bonding interactions. In a later report, this supramolecular strategy was successfully applied for the construction of J-aggregates for amine-substituted naphthalene-diimide by Fernández and Ghosh.[6] Nevertheless, only a very limited number of examples with intriguing properties resembling those of cyanine dye-based J-aggregates, *i.e.* the bathochromically shifted and sharpened narrower absorption band than that of the respective monomers and enhanced fluorescence with reduced lifetime, have been achieved so far.

Boron-dipyrromethene (BODIPY) dyes are a class of versatile organic chromophores and have attracted research interest in multiple fields.[7] The chemical structure of BODIPY dyes can be facilely modified, yielding products with improved optical and self-assembly properties.[8] Accordingly, considerable efforts have been devoted towards constructing supramolecular materials, *e.g.* organogels,[9] nanovesicles[10] and liquid crystals,[11] by using BODIPY as building blocks. However, while

[a]*School of Chemical Engineering and Technology, Tianjin University, Tianjin, 300072, China. E-mail: zjchen@tju.edu.cn, renxiangkui@tju.edu.cn*
[b]*Collaborative Innovation Center of Chemical Science and Chemical Engineering (Tianjin), Tianjin University, Tianjin, 300072, China*
†Electronic supplementary information (ESI) available. See DOI: 10.1039/d1qo00520k
‡These authors contributed equally to this work.

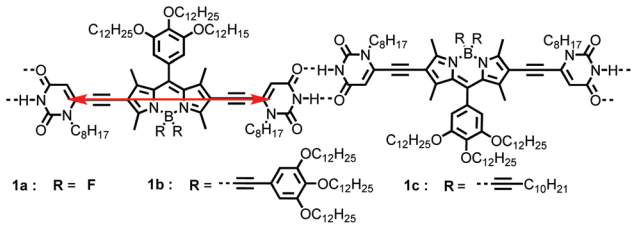

Scheme 1 J-aggregation pattern of uracil-functionalized BODIPYs **1a**, **1b**, and **1c** by H-bonding directed supramolecular polymerization along with the transition dipole moments (red arrow) of the dye molecules.

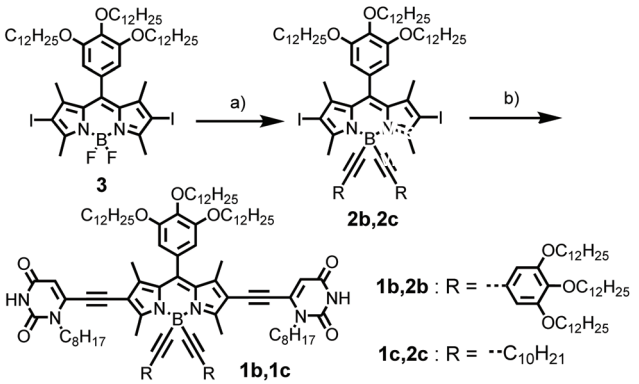

Scheme 2 The synthetic route for BODIPY dyes **1b**, **1c**. Reagents and conditions: (a) 3,4,5-Tridodecyloxyphenylacetylene (1-dodecyne), C_2H_5BrMg, THF, 60 °C, 6 h, 64%; (b) 6-ethynyl-1-*n*-octyluracil, $Pd(PPh_3)_4$, CuI, TEA, 70 °C, 4 h, 74%.

many BODIPY dyes exhibit high fluorescence quantum yields in dilute solutions, severe aggregation caused quenching (ACQ) of fluorescence may still take place,[12] even in the case when typical 1D J-aggregates were formed, as observed for the uracil-functionalized BODIPY dye **1a** (Scheme 1) in our previous report.[13] Thus, the development of dye assemblies of this class of BODIPYs without fluorescence quenching or with aggregation induced emission enhancement (AIEE)[14] is an appealing objective owing to their potential application in polarized luminescent materials[15] or in other fields.[16]

In the present work, we report two newly synthesized BODIPY dyes **1b** and **1c** and their emission enhancement induced by J-aggregation *via* supramolecular polymerization directed by H-bonding interactions between the uracil groups at both sides (2,6-positions) of the BODIPY core. Meanwhile, the dyes **1b** and **1c** have solubilizing moieties containing multiple alkyl chains at the *meso*-position of the BODIPY core and the boron atom, which improves the solubility of the dyes in aliphatic solvents compared with the fluorine-unsubstituted analogue dye **1a**. This feature is crucial for the supramolecular polymerization of **1b** and **1c** since it has been shown that the H-bonding interaction is much stronger in nonpolar aliphatic solvents, such as *n*-hexane, than in polar organic solvents.[17] The optical and structural properties of the supramolecular J-aggregates based on BODIPYs **1b** and **1c** were investigated by spectroscopic and microscopic measurements as well as molecular modelling to reveal the self-assembly mechanism and elucidate the observed strong AIEE effect for these J-aggregates.

Results and discussion

As shown in Scheme 2, the synthesis of BODIPY dyes **1b** and **1c** started from BODIPY **3** with iodo substituents at the 2,6-positions.[7b] Dye **3** was reacted with the Grignard reagents 3,4,5-tridodecyloxyphenylacetylene and 1-dodecyne to provide boron-substituted chromophores **2b** and **2c**, respectively. Subsequently, the 6-ethynyl-1-*n*-octyluracil units were appended on the 2,6-positions of the BODIPY core by Sonogashira coupling to give BODIPY dyes **1b** and **1c**.

The UV/Vis absorption spectrum of **1b** and **1c** in CH_2Cl_2 (c_T = 2.0 × 10^{-6} M) exhibits typical spectroscopic features for molecularly dissolved BODIPY dyes (Fig. 1a and Fig. S9†). For **1b**, the absorption band in the range of 540–600 nm was assigned to the S_0–S_1 transition band (ε = 1.5 × 10^5 M^{-1} cm^{-1} at 557 nm). The fluorescence spectrum of **1b** and **1c** in CH_2Cl_2

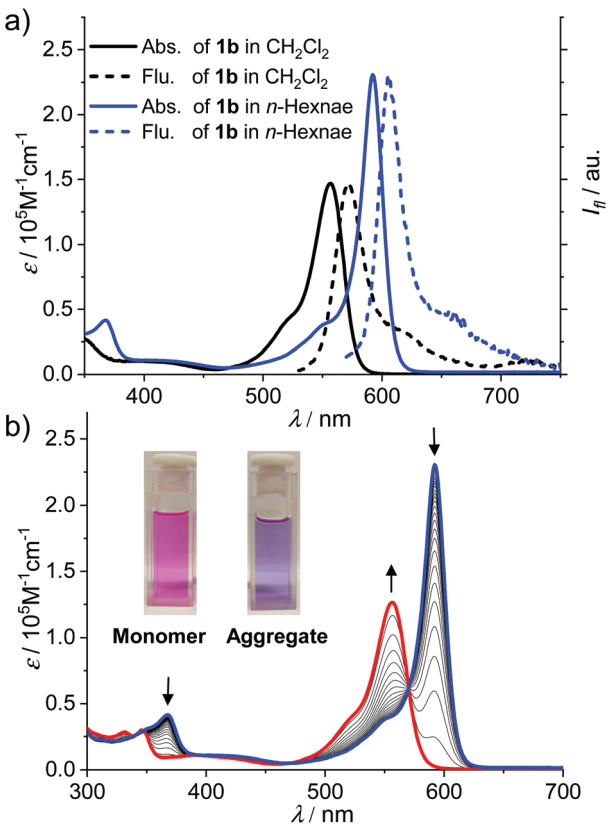

Fig. 1 (a) UV/Vis absorption and fluorescence spectra (λ_{Ex} = 350 nm) of dye **1b** in CH_2Cl_2 (black, c_T = 2.0 × 10^{-6} M) and *n*-hexane (blue, c_T = 2.0 × 10^{-6} M). (b) Temperature-dependent UV/Vis absorption spectra of BODIPY dye **1b** in *n*-hexane (c_T = 2.0 × 10^{-6} M). The arrows indicate the spectra changing with the increase of the temperature from 277 to 333 K. Inset: Visual appearance of solutions of monomeric and aggregated dye **1b** under daylight.

displayed a mirror-image relationship to the absorption spectrum. The absorption and emission spectra of **1b** and **1c** in CH_2Cl_2 are highly comparable, indicating that the different substituents at boron atoms have only minor effects on the spectroscopic properties. In CH_2Cl_2, the fluorescence quantum yields of the monomers of dyes **1b** and **1c** were determined to be 0.42 and 0.39, respectively.

For a solution of dye **1b** in *n*-hexane at the same concentration as in CH_2Cl_2 ($c_T = 2.0 \times 10^{-6}$ M), the spectral characteristics were obviously changed (Fig. 1a, blue lines). The maximum absorption wavelength (λ_{max}) of BODIPY dye **1b** in *n*-hexane was shifted bathochromically to 591 nm as compared with that in CH_2Cl_2 while the molar absorption coefficient at λ_{max} was largely increased to 2.4×10^5 M^{-1} cm^{-1}. Meanwhile, the band around 591 nm is obviously sharper than the S_0–S_1 band in DCM. Upon increasing the temperature of the solution in *n*-hexane (Fig. 1b), the absorption band of **1b** at 591 nm was gradually decreased while a new band at 556 nm arose, which resembled the S_0–S_1 transition band of the molecularly dissolved **1b** in CH_2Cl_2. In addition, an obvious colour change of the solution from purple (aggregate) to pink (monomer) was observed upon the increase in the temperature. All these observations pointed to the formation of J-aggregates of **1b** in nonpolar *n*-hexane.

The J-aggregation of **1b** in *n*-hexane was further confirmed by fluorescence spectroscopic measurements. As shown in Fig. 1a, the fluorescence spectrum displayed an approximately mirror-image relationship to the J-band with an emission maximum at 612 nm. Further temperature-dependent fluorescence spectra (Fig. 2a) indicated the gradual transition from the aggregated species to monomers upon heating. In addition, for the methylcyclohexane (MCH) solution of dye **1b** as well as the *n*-hexane and MCH solutions of dye **1c**, spectral characteristics of J-aggregates comparable with that for **1b** in *n*-hexane were observed (Fig. S10–S15†).

More interestingly, for both **1b** and **1c**, much brighter fluorescence could be observed by the naked eye for the J-aggregates than that of monomers under irradiation of UV light, implying the occurrence of AIEE for these dyes (Fig. 2a, insets). Accordingly, more photophysical properties, including concentration-dependent fluorescence quantum yields (Fig. S16†) and fluorescence lifetimes (Fig. 2b and Fig. S17–S20†), were measured for dyes **1b** and **1c** in *n*-hexane as well as MCH and the selected results are presented in Table 1. Indeed, the J-aggregates of **1b** and **1c** exhibit much higher fluorescence quantum yields than the monomers. For example, the fluorescence quantum yields of the monomers of **1b** in diluted *n*-hexane solutions ($c_T = 1.0 \times 10^{-7}$ M) were measured as 0.27. With the increase in the concentration, the fluorescence quantum yields of **1b** were gradually increased respectively to 0.62 ($c_T = 4.0 \times 10^{-6}$ M). Meanwhile, the concentration-dependent fluorescence spectra (Fig. S16b†) of **1b** exhibited bathochromically shifted emission bands that were characteristic of the formation of J-aggregates. Similar trends of the quantum yields at various concentrations were observed for these dyes in MCH. These results indicate explicitly the

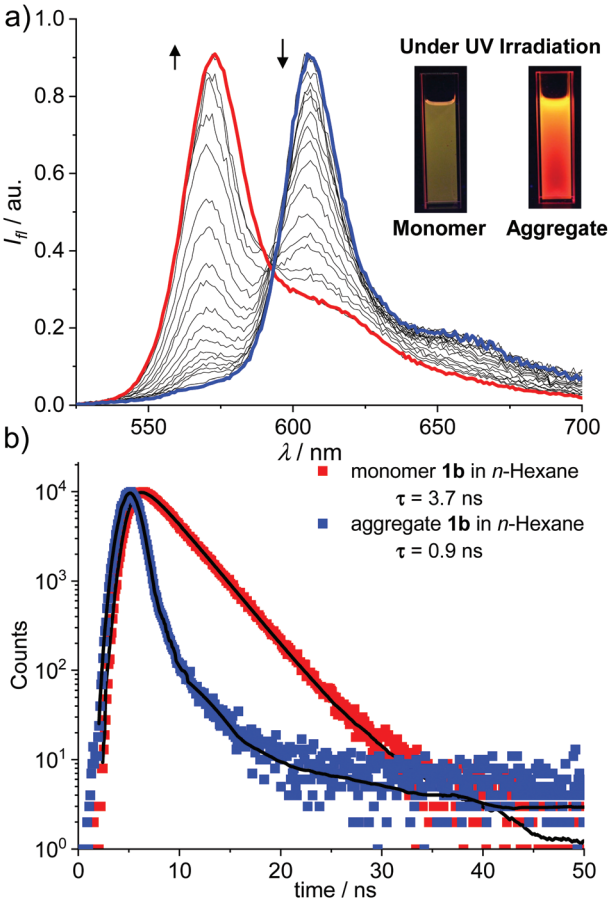

Fig. 2 (a) Temperature-dependent fluorescence spectra of **1b** in *n*-hexane ($c_T = 2.0 \times 10^{-6}$ M). The arrows indicate the spectra change with the increase in the temperature from 277 to 333 K. Inset: Visual appearance of solutions of monomeric and aggregated dye **1b** under a UV lamp (365 nm). (b) Time-resolved fluorescence decay for aggregates ($c_T = 1.0 \times 10^{-5}$ M, $\lambda_{Ex} = 350$ nm, $\lambda_{Em} = 612$ nm) and monomers ($c_T = 5.0 \times 10^{-8}$ M, $\lambda_{Ex} = 350$ nm, $\lambda_{Em} = 572$ nm) of **1b** in *n*-hexane.

J-aggregation induced emission enhancement properties of these dyes.

For the J-aggregates of dyes **1b** and **1c**, the pronounced bathochromic shifts in the absorption and emission spectra with an obviously narrowed band shape indicated the strong excitonic coupling interactions between the aggregated chromophores. For **1b**, distinct fluorescence lifetimes of 3.7 ns and 0.9 ns were measured for monomers and J-aggregates in *n*-hexane, respectively. The decreased fluorescence lifetime is indicative of enhanced radiative decay arising from the excitonic coherence between the aggregated molecules. To estimate the size of the coherent domain in J-aggregates, the radiative decay rate constants (k_r) were calculated from $k_r = \Phi/\tau$. Thus, $k_r^J = 6.8 \times 10^8$ s^{-1} and $k_r^M = 7.3 \times 10^7$ s^{-1} were evaluated for J-aggregates and monomers of **1b** respectively. Furthermore, a coherent size[18] of $N \approx 9$ for J-aggregates of **1b** can be estimated with $N = k_r^J/k_r^M$. Similarly, the coherent size in J-aggregates of **1c** in *n*-hexane can be estimated to be *ca.* 4 dye molecules. These results confirmed that the AIEE property of

Table 1 UV/Vis absorption and fluorescence spectroscopic properties of BODIPY dyes **1b** and **1c** including the maximum absorption and emission wavelengths for monomers (λ_{mon} and $\lambda_{em,mon}$) and for aggregates (λ_{agg} and $\lambda_{em,agg}$) as well as the fluorescence quantum yields and lifetimes for monomers (Φ_{mon} and τ_{mon}) and for aggregates (Φ_{agg} and τ_{agg})

Dyes	Solvent	λ_{mon}/nm	λ_{agg}/nm	$\lambda_{em,mon}$/nm	$\lambda_{em,agg}$/nm	Φ_{mon}	Φ_{agg}	τ_{mon}/ns	τ_{agg}/ns
1b	CH_2Cl_2	557	N/A	578	N/A	0.42	N/A	3.9	N/A
1c	CH_2Cl_2	555	N/A	568	N/A	0.39	N/A	4.5	N/A
1b	*n*-Hexane	556	591	572	612	0.27	0.62	3.7	0.9
1c	*n*-Hexane	555	590	570	604	0.19	0.51	3.4	2.4
1b	MCH	559	588	578	608	0.39	0.58	3.0	2.1
1c	MCH	558	589	570	603	0.23	0.48	3.2	2.5

J-aggregates of **1b** and **1c** is mainly caused by a superradiance effect. It is worth noting that the mechanism of J-aggregation induced emission enhancement observed for dyes **1b** and **1c** is obviously different from that of the other AIEgens such as tetraphenylethene and silole derivatives, for which a mechanism of restriction of intramolecular rotation (RIR) has been proposed to explain the enhancement of fluorescence.[19]

To give further insights into the mechanistic and structural aspects of the supramolecular polymerization of uracil-functionalized BODIPY dyes **1b** and **1c**, detailed analysis of the spectroscopic data as well as morphological studies of the J-aggregates were carried out. Based on the temperature-dependent UV/Vis spectroscopic data (Fig. 1b and Fig. S10–S12†), the fraction of aggregated molecules (α_{agg}) *versus* temperature (T) was evaluated (for details, see the ESI†) and further fitted with the nucleation–elongation supramolecular polymerization model (Fig. 3a).[20] The α_{agg}–T plots exhibited satisfactory accordance with cooperative processes. For the aggregation process of **1b** in *n*-hexane (c_T = 2.0 × 10^{-6} M), the critical elongation temperature (T_e) and molar enthalpy (ΔH_e) were determined to be 330 K and −74.2 kJ mol^{-1} respectively (Table 2). For dye **1c**, lower T_e (318 K) and ΔH_e (−64.5 kJ mol^{-1}) were obtained at the same concentration, which indicates that **1b** has a stronger tendency for aggregation. The dimensionless equilibrium constants (K_a) of the activation step at T_e were determined to be 1.5 × 10^{-3} and 8.7 × 10^{-4} for **1b** and **1c** respectively, implying a higher degree of cooperativity for the aggregation process of **1b**. As a comparison, the fitting results of the α_{agg}–T plots in MCH (c_T = 1.0 × 10^{-5} M) gave a similar trend to that in *n*-hexane, *i.e.*, **1b** possesses a higher T_e and a smaller ΔH_e than **1c** (Table 2).

Moreover, concentration-dependent UV/Vis absorption spectroscopic investigation was performed for BODIPY dyes **1b** and **1c** and spectral changes comparable with those in temperature-dependent studies were observed (Fig. S21 and S22†). By fitting the experimental data of α_{agg} *versus* concentration c_T with the Goldstein–Stryer model for nucleated supramolecular polymerization (Fig. 3),[17b,21] parameters including nucleus size s, cooperativity factor σ and the elongation equilibrium constant K_E were obtained (Table 2). These results corroborate the cooperative mechanism of the self-assembly processes of **1b** and **1c**. For **1b**, the aggregates in *n*-hexane could not fully disaggregate to monomers at 298 K even upon diluting to a concentration of 1.0 × 10^{-7} M. Thus, the equilibrium constant

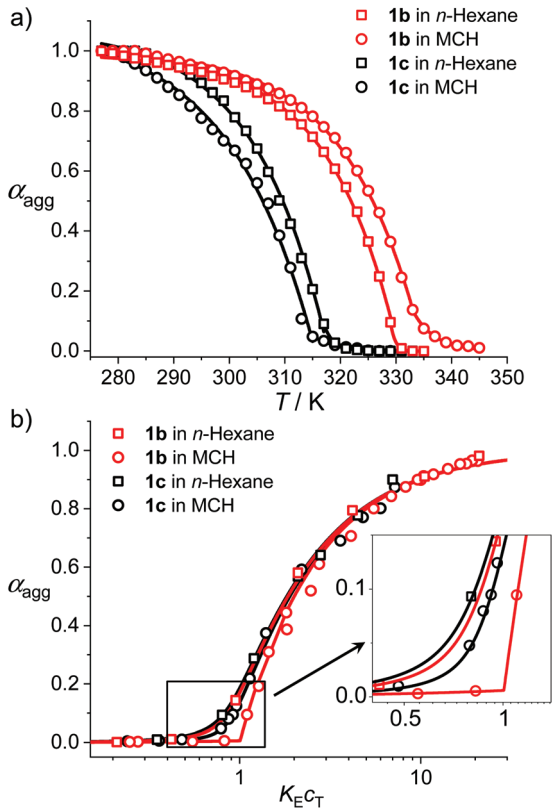

Fig. 3 (a) Plot of the molar fraction of aggregated molecules of **1b** and **1c** in *n*-hexane (c_T = 2.0 × 10^{-6} M) and MCH (c_T = 1.0 × 10^{-5} M) as a function of the temperature and the fitting curves by applying the cooperative self-assembly model. (b) Plot of the molar fraction of aggregated molecules of **1b** and **1c** in *n*-hexane and MCH as a function of the dimensionless concentration $K_E c_T$ and fitting curves by applying the Goldstein–Stryer model.

of **1b** in *n*-hexane was measured at 313 K and a K_E of 2.1 × 10^6 M^{-1} was obtained. In MCH, the K_E for the self-assembly of dye **1b** is higher than that obtained for **1c**, indicating that the aggregates of **1b** have higher stability, which is consistent with the temperature-dependent spectroscopic studies. Moreover, the K_E values of **1b** and **1c** in *n*-hexane are one order of magnitude higher than those in MCH, which is rational since the relatively less polar *n*-hexane is beneficial for the intermolecular H-bonding interaction.[22]

Table 2 Thermodynamic parameters for the self-assembly of **1b** and **1c** including the critical elongation temperature (T_e), molar enthalpy (ΔH_e) and dimensionless equilibrium constant (K_a) obtained from temperature-dependent UV/Vis studies as well as the cooperativity factor (σ), the nucleus size (s) and the elongation equilibrium constant (K_E) obtained from concentration-dependent UV/Vis studies

Dyes	T_e/K	ΔH_e/kJ mol^{-1}	K_a	σ^c	s^c	$K_E{}^c/10^6$ M^{-1}
1b [a]	330	−74.2	1.5×10^{-3}	0.006	2	2.1
1b [b]	334	−69.7	3.2×10^{-4}	0.003	3	0.28
1c [a]	318	−64.5	8.7×10^{-4}	0.008	2	3.5
1c [b]	315	−54.4	8.9×10^{-5}	0.003	2	0.12

[a] Measured in *n*-hexane. [b] Measured in MCH. [c] Data of **1b** in *n*-hexane are measured at $T = 313$ K while data of **1b** in MCH and **1c** in both solvents are measured at $T = 298$ K.

The H-bonding interactions between the 2,6-uracil groups of adjacent dye molecules were characterized by concentration-dependent ^{1}H NMR spectroscopy (Fig. S23 and 24†) in $CDCl_3$. For both dyes, significant concentration-dependency was observed for the signal of imide-H. As shown by **1b**, the signal of imide-H displayed a constant downfield shift from 7.9 to 8.9 ppm while the dye concentration was gradually increased from of 9.8×10^{-5} M to 1.3×10^{-2} M, indicating the formation of intermolecular hydrogen bonds between uracil groups. According to a model developed by LaPlanche *et al.*,[23] association constants of 410 M^{-1} and 450 M^{-1} in $CDCl_3$ were obtained respectively for the H-bonding of dyes **1b** and **1c**. The nearly identical association constants for the two dyes suggested that the substituents at boron atoms have a minor effect on the H-bonding interactions. The H-bonding directed supramolecular polymerization often leads to the formation of 1D nanostructures, such as nanowires or nanofibers.[24] Accordingly, the nanomorphology of the J-aggregates for BODIPY dyes **1b** and **1c** was characterized by atomic force microscopy (AFM). The results indicated that **1b** self-assembled into nanowires with a width over 100 nm and a height of *ca.* 4 nm (Fig. 4). The J-aggregates of **1c** exhibited a morphology similar to that of nanowires with a width of *ca.* 50 nm and a height of *ca.* 3 nm.

Based on mechanistic analysis and the structural characterization for the J-aggregates of BODIPY **1b** and **1c**, a schematic illustration of the supramolecular polymerization process and molecular packing is proposed, as shown in Fig. 4c. Driven by the complementary intermolecular H-bonding interactions, the dimeric nucleus was first formed in the nucleation process and a subsequent elongation process gave the 1D H-bonding polymers in solution. Accordingly, highly "slipped" J-type arrangement of the transition dipole moments was obtained, as indicated by the large bathochromic shifts for these aggregates in absorption and emission spectroscopic measurements.

To shed more light on the observed J-aggregation induced emission enhancement for **1b** and **1c**, molecular modelling and calculations based on molecular exciton theory were performed to elucidate the molecular arrangement in the

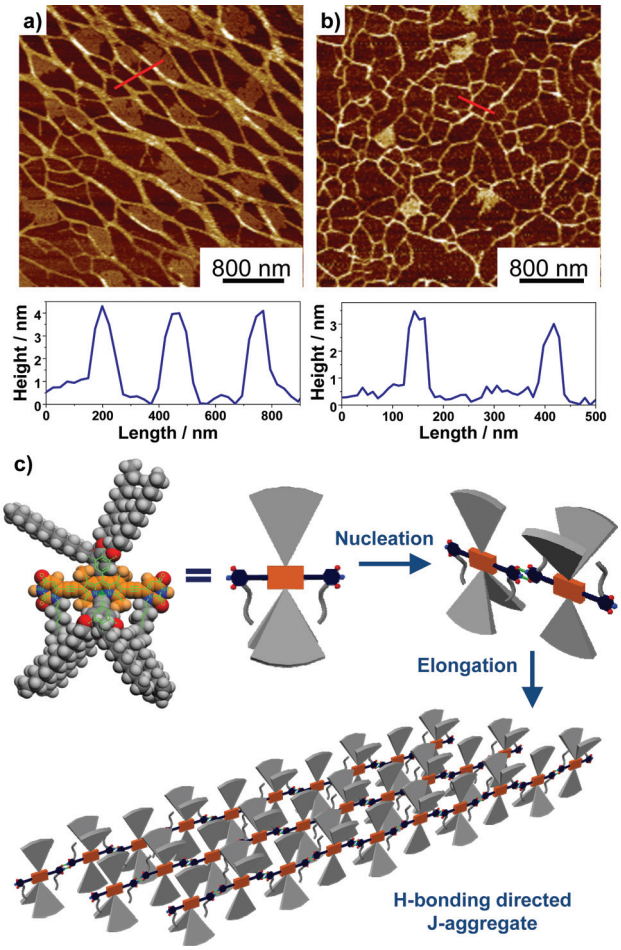

Fig. 4 AFM images of J-aggregates of BODIPY dyes (a) **1b** and (b) **1c** by drop-casting *n*-hexane solution ($c_T = 1.0 \times 10^{-5}$ M) on the mica surface and cross-section analysis along the red lines. (c) Schematic illustration of the formation of elongated 1D J-aggregates through the nucleation–elongation mechanism.

J-aggregates of these dyes. For the geometry-optimized tetrameric aggregates of **1a–c** (Fig. 5 and Fig. S25†), it was observed that the π–π distances between the planes of dipyrromethene cores are significantly varied, confirming the difference in the molecular arrangement for the J-aggregates of dyes **1a–c**. The chromophores of **1a** exhibit close π–π stacking with a distance of about 0.46 nm, whereas for **1b** and **1c**, this distance increased to 0.88 and 0.75 nm, respectively. Meanwhile, the experimental bathochromic shift of the absorption band for **1a** (−1469 cm^{-1}) is obviously larger than that for **1b** and **1c** (−895 cm^{-1} and −957 cm^{-1}), implying the stronger excitonic coupling interactions of **1a** in the π–π-stacking direction since the center-to-center distance along the H-bonding direction of the chromophores should be nearly identical for these dyes (*vide infra*).

Furthermore, the spectral shift of the absorption band upon J-aggregation was estimated by Kasha's molecular exciton theory[25] based on the molecular modelling results. A "brickwork" model is proposed for the molecular arrangement

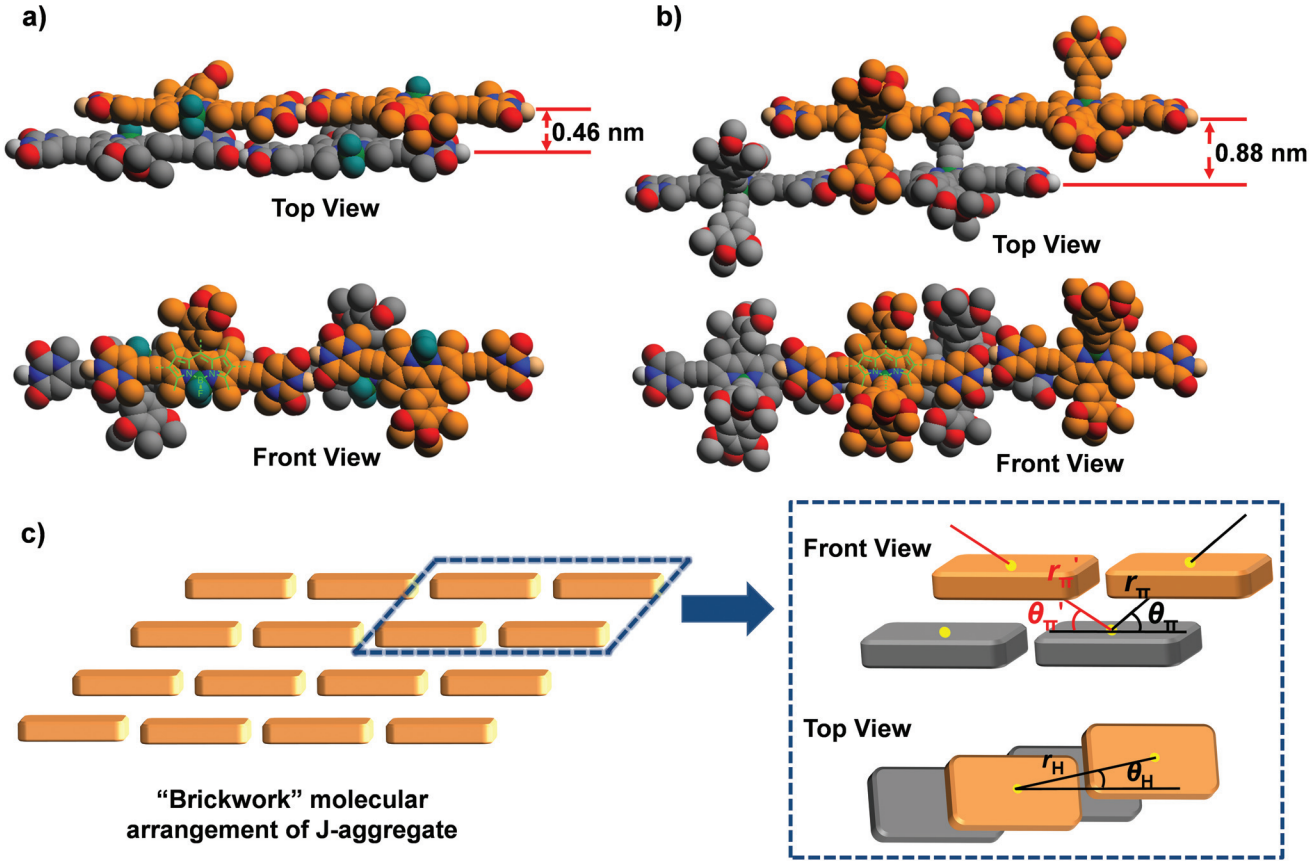

Fig. 5 Geometrically optimized tetrameric aggregates for dyes (a) **1a** and (b) **1b** with the PM6-D3H4 method (for clarity, alkyls and hydrogen atoms are omitted and the molecules are shown in grey and orange colours). (c) Schematic representation of the "brickwork" model and the geometrical parameters that are considered for theoretical calculations with molecular exciton theory.

in J-aggregates of **1a–c** (Fig. 5c), in which only the nearest neighbour interactions were considered. Accordingly, one molecule had excitonic coupling interactions with two H-bonded neighbouring molecules and four π–π stacked ones. The geometrical parameters for the estimation of spectral shift in a "brickwork" model are presented in Fig. 5c, where the parameters r_H and r_π/r'_π refer to the center-to-center distances between two H-bonded or π–π stacked chromophores respectively while θ_H and θ_π/θ'_π refer to the angles defined by the direction of the transition dipole moment of one chromophore and the line connecting the centers of two neighbouring chromophores. These geometrical parameters for the J-aggregation of dyes **1a–c** were obtained from the structure-optimized tetrameric aggregates and are listed in Table 3. As a result, the spectral shifts for J-aggregation of **1a–c** are estimated as $\Delta\tilde{\nu} \leq -1371$ cm^{-1}, $\Delta\tilde{\nu} \leq -895$ cm^{-1}, and $\Delta\tilde{\nu} \leq -957$ cm^{-1} respectively (for details, see the ESI†), which are consistent with the experimental data of these dyes obtained from UV/Vis spectroscopic measurements. In the π–π-stacking directions, the calculated $\Delta\tilde{\nu}$ of **1b** and **1c** (-718 cm^{-1} and -822 cm^{-1}) are much lower than that for **1a** (-1276 cm^{-1}), indicating that the bulky substituents on boron can cause considerable steric hindrance to suppress the excitonic interactions in the π–π stacking directions. Considering the ACQ and AIEE effects observed for the J-aggregates of **1a** and **1b** & **1c** respectively, one can speculate that the segregation effect of bulky substituent groups is crucial to prevent the close π–π contact as well as ACQ of chromophores and lead to the J-aggregation-induced emission enhancement for dyes **1b** and **1c**.

Table 3 The transition dipole moment of the monomers (μ_{eg}), geometrical parameters for molecular arrangements in J-aggregates of dyes **1a–c** from molecular modelling, and the calculated and experimental spectral shifts ($\Delta\tilde{\nu}_{cal}$ and $\Delta\tilde{\nu}_{ex}$)

Dyes	μ_{eg}/D	r_H/Å	θ_H/°	r_π/Å	θ_π/°	r'_π/Å	θ'_π/°	$\Delta\tilde{\nu}_{cal}$/cm^{-1}	$\Delta\tilde{\nu}_{ex}$/cm^{-1}
BODIPY **1a**	7.9	23.6	6.0	8.1	37.3	17.3	15.5	−1371	−1469
BODIPY **1b**	10.9	23.7	5.2	17.2	30.7	12.6	40.7	−895	−1065
BODIPY **1c**	9.4	23.4	5.7	13.3	34.3	13.1	33.7	−957	−1069

Conclusions

In this work, two new uracil-functionalized BODIPY dyes **1b** and **1c** modified with bulky substituents on the boron atom were synthesized and characterized. Through supramolecular polymerization directed by intermolecular H-bonding interactions between the uracil groups, these dyes assembled into 1D J-aggregates with intense, bathochromically shifted absorption and fluorescence bands in nonpolar solvents *n*-hexane and MCH. Temperature- and concentration-dependent spectroscopic studies revealed the cooperative supramolecular polymerization of **1b** and **1c** with a nucleation–elongation mechanism. Moreover, the fluorescence quantum yields of J-aggregates of **1b** and **1c** were found to be significantly higher than that of the monomers, indicating extraordinary AIEE properties that could be ascribed to the excitonic coupling between aggregated molecules. Further structural characterization revealed that the dyes **1b** and **1c** supramolecularly polymerized into nanowires through intermolecular H-bonding interactions. Meanwhile, molecular modelling and calculations based on exciton theory indicated that the bulky substituent groups appended on boron atoms were able to largely hinder the close contact between the π-faces of BODIPY chromophores **1b** and **1c**. Accordingly, the combination of H-bonding interactions along the transition dipole moments and appropriate segregation of supramolecular polymer chains was demonstrated to be an effective strategy for the design of dye building blocks exhibiting both J-aggregation and AIEE properties.

Conflicts of interest

There are no conflicts to declare.

Acknowledgements

This work is supported by the National Natural Science Foundation of China (no. 92056115 and 21875157).

Notes and references

1 (*a*) E. E. Jelley, Spectral absorption and fluorescence of dyes in the molecular state, *Nature*, 1936, **138**, 1009; (*b*) H. von Berlepsch, C. Böttcher and L. Dähne, Structure of J-aggregates of pseudoisocyanine dye in aqueous solution, *J. Phys. Chem. B*, 2000, **104**, 8792; (*c*) T. E. Kaiser, V. Stepanenko and F. Würthner, Fluorescent J-Aggregates of Core-Substituted Perylene Bisimides: Studies on Structure-Property Relationship, Nucleation-Elongation Mechanism, and Sergeants-and-Soldiers Principle, *J. Am. Chem. Soc.*, 2009, **131**, 6719; (*d*) F. Würthner, T. E. Kaiser and C. R. Saha-Möeller, J-Aggregates: From Serendipitous Discovery to Supramolecular Engineering of Functional Dye Materials, *Angew. Chem., Int. Ed.*, 2011, **50**, 3376.

2 S. Kirstein and S. Dähne, J-aggregates of amphiphilic cyanine dyes: Self-organization of artificial light harvesting complexes, *Int. J. Photoenergy*, 2006, **2006**, 1.

3 (*a*) M. T. Spitler, Dye Photo-Oxidation at Semiconductor Electrodes-A Corollary to Spectral Sensitization in Photography, *J. Chem. Educ.*, 1983, **60**, 330; (*b*) C. Nasr, D. Liu, S. Hotchandani and P. V. Kamat, Dye-capped semiconductor nanoclusters. Excited state and photosensitization aspects of rhodamine 6G H-aggregates bound to SiO_2 and SnO_2 colloids, *J. Phys. Chem.*, 1996, **100**, 11054.

4 H. von Berlepsch, S. Kirstein, R. Hania, A. Pugzlys and C. Böttcher, Modification of the nanoscale structure of the J-aggregate of a sulfonate-substituted amphiphilic carbocyanine dye through incorporation of surface-active additives, *J. Phys. Chem. B*, 2007, **111**, 1701.

5 (*a*) T. E. Kaiser, H. Wang, V. Stepanenko and F. Würthner, Supramolecular construction of fluorescent J-aggregates based on hydrogen-bonded perylene dyes, *Angew. Chem., Int. Ed.*, 2007, **46**, 5541; (*b*) Z. Xie, V. Stepanenko, K. Radacki and F. Würthner, Chiral J-Aggregates of Atropo-Enantiomeric Perylene Bisimides and Their Self-Sorting Behavior, *Chem. – Eur. J.*, 2012, **18**, 7060; (*c*) F. Fennel, J. Gershberg, M. Stolte and F. Würthner, Fluorescence quantum yields of dye aggregates: a showcase example based on self-assembled perylene bisimide dimers, *Phys. Chem. Chem. Phys.*, 2018, **20**, 7612.

6 (*a*) H. Kar, D. W. Gehrig, N. K. Allampally, G. Fernández, F. Laquai and S. Ghosh, Cooperative supramolecular polymerization of an amine-substituted naphthalenediimide and its impact on excited state photophysical properties, *Chem. Sci.*, 2016, **7**, 1115; (*b*) H. Kar and S. Ghosh, J-aggregation of a sulfur-substituted naphthalenediimide (NDI) with remarkably bright fluorescence, *Chem. Commun.*, 2016, **52**, 8818.

7 (*a*) G. Fan, Y. Lin, L. Yang, F. Gao, Y. Zhao, Z. Qiao, Q. Zhao, Y. Fan, Z. Chen and H. Wang, Co-self-assembled nanoaggregates of BODIPY amphiphiles for dual colour imaging of live cells, *Chem. Commun.*, 2015, **51**, 12447; (*b*) L. Yang, G. Fan, X. Ren, L. Zhao, J. Wang and Z. Chen, Aqueous self-assembly of a charged BODIPY amphiphile via nucleation-growth mechanism, *Phys. Chem. Chem. Phys.*, 2015, **17**, 9167; (*c*) N. Boens, V. Leen and W. Dehaen, Fluorescent indicators based on BODIPY, *Chem. Soc. Rev.*, 2012, **41**, 1130; (*d*) E. V. Antina, N. A. Bumagina, A. V'Yugin and A. V. Solomonov, Fluorescent indicators of metal ions based on dipyrromethene platform, *Dyes Pigm.*, 2017, **136**, 368.

8 (*a*) A. Loudet and K. Burgess, BODIPY dyes and their derivatives: Syntheses and spectroscopic properties, *Chem. Rev.*, 2007, **107**, 4891; (*b*) L. Niu, Y. Guan, Y. Chen, L. Wu, C. Tung and Q. Yang, BODIPY-Based Ratiometric Fluorescent Sensor for Highly Selective Detection of Glutathione over Cysteine and Homocysteine, *J. Am. Chem. Soc.*, 2012, **134**, 18928; (*c*) H. Lu, J. Mack, Y. Yang and Z. Shen, Structural modification strategies for the rational design of red/NIR region BODIPYs, *Chem. Soc. Rev.*, 2014,

43, 4778; (*d*) T. Kowada, H. Maeda and K. Kikuchi, BODIPY-based probes for the fluorescence imaging of biomolecules in living cells, *Chem. Soc. Rev.*, 2015, **44**, 4953.

9 F. Camerel, L. Bonardi, G. Ulrich, L. Charbonniere, B. Donnio, C. Bourgogne, D. Guillon, P. Retailleau and R. Ziessel, Self-assembly of fluorescent amphipathic boron-dipyrromethene scaffoldings in mesophases and organogels, *Chem. Mater.*, 2006, **18**, 5009.

10 A. Nagai, K. Kokado, J. Miyake and Y. Cyujo, Thermoresponsive Fluorescent Water-Soluble Copolymers Containing BODIPY Dye: Inhibition of H-Aggregation of the BODIPY Units in Their Copolymers by LCST, *J. Polym. Sci., Part A: Polym. Chem.*, 2010, **48**, 627.

11 (*a*) J.-H. Oliver, F. Camerel, G. Ulrich, J. Barbera and R. Ziessel, Luminescent Ionic Liquid Crystals from Self-Assembled BODIPY Disulfonate and Imidazolium Frameworks, *Chem. – Eur. J.*, 2010, **16**, 7134; (*b*) M. Benstead, G. A. Rosser, A. Beeby, G. H. Mehl and R. W. Boyle, Mesogenic BODIPYs: an investigation of the correlation between liquid crystalline behaviour and fluorescence intensity, *Photochem. Photobiol. Sci.*, 2011, **10**, 992.

12 Y. Tokoro, A. Nagai and Y. Chujo, Nanoparticles via H-aggregation of amphiphilic BODIPY dyes, *Tetrahedron Lett.*, 2010, **51**, 3451.

13 Y. Zhang, P. Liu, H. Pan, H. Dai, X. K. Ren and Z. Chen, Alignment of supramolecular J-aggregates based on uracil-functionalized BODIPY dye for polarized photoluminescence, *Chem. Commun.*, 2020, **56**, 12069.

14 (*a*) S. Choi, J. Bouffard and Y. Kim, Aggregation-induced emission enhancement of a meso-trifluoromethyl BODIPY via J-aggregation, *Chem. Sci.*, 2014, **5**, 751; (*b*) S. Kim, J. Bouffard and Y. Kim, Tailoring the Solid-State Fluorescence Emission of BODIPY Dyes by meso Substitution, *Chem. – Eur. J.*, 2015, **21**, 17459; (*c*) Z. Liu, Z. Jiang, M. Yan and X. Wang, Recent Progress of BODIPY Dyes With Aggregation-Induced Emission, *Front. Chem.*, 2019, **7**, 712.

15 J. Koo, S. I. Lim, S. H. Lee, J. S. Kim, Y. T. Yu, C. R. Lee, D. Y. Kim and K. U. Jeong, Polarized Light Emission from Uniaxially Oriented and Polymer-Stabilized AIE Luminogen Thin Films, *Macromolecules*, 2019, **52**, 1739.

16 (*a*) A. C. Benniston and G. Copley, Lighting the way ahead with boron dipyrromethene (Bodipy) dyes, *Phys. Chem. Chem. Phys.*, 2009, **11**, 4124; (*b*) S. Lim, M. M. Haque, D. Su, D. Kim, J.-S. Lee, Y.-T. Chang and Y. K. Kim, Development of a BODIPY-based fluorescent probe for imaging pathological tau aggregates in live cells, *Chem. Commun.*, 2017, **53**, 1607.

17 (*a*) M. S. Cubberley and B. L. Iverson, H-1 NMR investigation of solvent effects in aromatic stacking interactions, *J. Am. Chem. Soc.*, 2001, **123**, 7560; (*b*) Z. Chen, A. Lohr, C. R. Saha-Moeller and F. Würthner, Self-assembled pi-stacks of functional dyes in solution: structural and thermodynamic features, *Chem. Soc. Rev.*, 2009, **38**, 564.

18 H. Wang, T. E. Kaiser, S. Uernura and F. Würthner, Perylene bisimide J-aggregates with absorption maxima in the NIR, *Chem. Commun.*, 2008, **10**, 1181.

19 (*a*) R. Hu, E. Lager, A. Aguilar-Aguilar, J. Liu, J. W. Y. Lam, H. H. Y. Sung, I. D. Williams, Y. Zhong, K. S. Wong, E. Pena-Cabrera and B. Z. Tang, Twisted Intramolecular Charge Transfer and Aggregation-Induced Emission of BODIPY Derivatives, *J. Phys. Chem. C*, 2009, **113**, 15845; (*b*) Y. Hong, J. W. Lam and B. Z. Tang, Aggregation-induced emission, *Chem. Soc. Rev.*, 2011, **40**, 5361; (*c*) R. Hu, N. L. C. Leung and B. Z. Tang, AIE macromolecules: syntheses, structures and functionalities, *Chem. Soc. Rev.*, 2014, **43**, 4494; (*d*) R. Hu, A. Qin and B. Z. Tang, AIE polymers: Synthesis and applications, *Prog. Polym. Sci.*, 2020, **100**, 101176.

20 (*a*) P. Jonkheijm, P. van der Schoot, A. P. H. J. Schenning and E. W. Meijer, Probing the solvent-assisted nucleation pathway in chemical self-assembly, *Science*, 2006, **313**, 80; (*b*) M. M. J. Smulders, A. P. H. J. Schenning and E. W. Meijer, Insight into the mechanisms of cooperative self-assembly: The "sergeants-and-soldiers" principle of chiral and achiral C-3-symmetrical discotic triamides, *J. Am. Chem. Soc.*, 2008, **130**, 606.

21 R. F. Goldstein and L. Stryer, Cooperative Polymerization Reactions-Analytical Approximations, Numerical Examples, and Experimental Strategy, *Biophys. J.*, 1986, **50**, 583.

22 S. K. Yang and S. C. Zimmerman, Hydrogen Bonding Modules for Use in Supramolecular Polymers, *Isr. J. Chem.*, 2013, **53**, 511.

23 (*a*) L. A. LaPlanche, H. B. Thompson and M. T. Rogers, Chain AssociationEquilibria. A Nuclear Magnetic Resonance Study of the Hydrogen Bonding of N-Monosubstituted Amides, *J. Phys. Chem.*, 1964, **69**, 1482; (*b*) W. S. Horne, C. D. Stout and M. R. Ghadiri, A heterocyclic peptide nanotube, *J. Am. Chem. Soc.*, 2003, **125**, 9372.

24 O. J. G. M. Goor, S. I. S. Hendrikse, P. Y. W. Dankers and E. W. Meijer, From supramolecular polymers to multi-component biomaterials, *Chem. Soc. Rev.*, 2017, **46**, 6621.

25 M. Kasha, H. R. Rawls and M. A. El-Bayoumi, The exciton model in molecular spectroscopy, *Pure Appl. Chem.*, 1965, **11**, 371.